

Modification of Li Anode with Perfluorodecyltrimethoxysilane to Enhance the Performance of Lithium Metal Battery

Yinghan Shao*

Institute of Problem Solving, Bond International College, Toronto, Canada

Email: *shaoyinghan00@gmail.com

How to cite this paper: Shao, Y.H. (2024) Modification of Li Anode with Perfluorodecyltrimethoxysilane to Enhance the Performance of Lithium Metal Battery. *Journal of Power and Energy Engineering*, 12, 70-77. <https://doi.org/10.4236/jpee.2024.128005>

Received: July 4, 2024

Accepted: August 27, 2024

Published: August 30, 2024

Copyright © 2024 by author(s) and Scientific Research Publishing Inc. This work is licensed under the Creative Commons Attribution International License (CC BY 4.0).

<http://creativecommons.org/licenses/by/4.0/>



Open Access

Abstract

The solid electrolyte interphase (SEI) on the surface of lithium metal anodes can dictate the electrochemical performance of lithium-metal-based batteries. Due to ineffective adhesion, the natural SEI layer may detach from the lithium negative electrode during interface fluctuations, thereby deteriorating the electrochemical performance of lithium-metal-based batteries. This work introduces perfluorosiloxane coupling agents as interfacial adhesion promoters, chemically bonding and physically entangling the lithium metal with the SEI via the formation of Li-O-Si bonds with the inorganic reactive groups anchoring to the Li substrate and the organic functional groups participating in the formation of the SEI layer, thus binding with its components. Lithium metal batteries modified with silane coupling agents exhibit superior electrochemical performance compared to unmodified lithium metal batteries. The modified lithium metal battery retains a specific capacity of 162 mAh/g after 200 cycles, while the unmodified lithium metal battery only retains 140 mAh/g.

Keywords

Lithium Metal Battery, SEI, High Density, PFDTMS, Surface

1. Introduction

Lithium metal, with its ultra-high theoretical specific capacity (3860 mAh g^{-1}) and low reduction potential (3.04 V versus the standard hydrogen electrode), is widely regarded as the ideal anode material for next-generation batteries [1]-[3]. However, the intrinsic drawbacks of the lithium metal anode have significantly

hindered its commercial adoption. Lithium metal is unstable in non-aqueous solvents, leading to a continuous series of chemical reactions until a passivating solid electrolyte interphase (SEI) layer forms on the lithium surface [4]. During Li plating/stripping, this layer becomes mechanically unstable under substantial interfacial fluctuations, constantly cracking and reforming, consuming the Li anode and electrolyte [5]. More problematically, the primary hazard in lithium-metal-based batteries arises from lithium dendrites that readily grow out of cracks in the SEI layer [4]. Operando scanning transmission electron microscopy observations reveal damage to the SEI layer during these interfacial fluctuations, ultimately resulting in its detachment, leaving an unprotected electrode surface exposed to the electrolyte [6]. The detachment of the SEI layer can be attributed to the poor chemical adhesion between the SEI layer and the Li substrate. Clearly, a stable and robust SEI layer is the determining factor for safe, dendrite-free, and long-life lithium-metal-based batteries [7]. To optimize the SEI layer, researchers have developed functional additives, novel solvents, and high-concentration electrolytes to in situ adjust its composition and structure. Reinforcement of the SEI layer can also be achieved through non-in situ coating protective layers, such as Nafion [8], hexagonal boron nitride (h-BN) [9], LiF [10] [11], and Li_3PO_4 [12]. While various strategies have been proposed, these studies primarily focus on the performance of the SEI layer itself, with minimal attention given to the bond between the SEI layer and the Li metal substrate.

To address the challenge of the unstable SEI interface, herein we devise a simple yet effective approach to achieve SEI reinforcement through the use of perfluorodecyltrimethoxysilane (PFDTMS) coupling agent. The concept is inspired by the remarkable ability of plant cell walls to selectively block the intrusion of foreign bacteria while facilitating the infiltration of essential nutrients, demonstrating a sophisticated balance between protection and permeability. Coating lithium metal surfaces with PFDTMS serves a similar purpose, protecting the metal lithium from electrolyte attack while still allowing for the free deposition of lithium ions. Commercial Li foil is immersed in a solution containing PFDTMS, whereupon the PFDTMS molecules spontaneously graft onto the Li foil surface, assembling into a thin, dense layer designated as the PFDTMS layer. This layer adheres firmly to the lithium metal surface via the formation of covalent bonds (Li-O-Si) and connects to the SEI layer through a combination of chemical bonding and physical entanglement effects. Consequently, an effective linkage between the dissimilar materials of Li metal and the SEI layer is established. The PFDTMS-modified lithium metal foil (PFDTMS-Li) exhibits enhanced adhesion and remarkable electrochemical performance. PFDTMS-Li||PFDTMS-Li symmetric cells demonstrate stable cycling for 600 hours at a current density and capacity density of 0.5 mA cm^{-2} and 0.5 mAh cm^{-2} , respectively, whereas the Li||Li cell gradually fails due to polarization after cycling to 300 hours. Even with high mass loading of cathode material and limited electrolyte, the PFDTMS-Li||lithium iron phosphate (LFP) full cell retains a capacity of 162 mAh g^{-1} after 200 cycles at a current density of 1 C.

2. Experimental Section

Preparation of PFDTMS@Li Composite. In a typical synthesis procedure for fabricating the PFDTMS@Li composite, lithium sheets were homogeneously dispersed within a 20 mL solution containing 0.1 wt% of PFDTMS dissolved in tetrahydrofuran (THF). This dispersion was achieved through vigorous magnetic stirring, which ensured a uniform distribution of the lithium within the PFDTMS-THF mixture over the course of several minutes. Following the stirring process, the resultant slurry underwent multiple rinses with fresh THF to remove any unreacted or loosely bound components. To finalize the synthesis and remove any residual solvents, the composite was subjected to a drying process. This involved placing it in a vacuum oven at an elevated temperature of 333 K for a duration of 10 hours. This extended drying period under vacuum conditions facilitated the complete evaporation of any remaining THF, ensuring that the final product was free from solvent impurities and ready for further characterization or use.

Electrochemical Characterization. For the assembly of batteries intended for electrochemical measurements, CR2025-type coin cells were employed. These cells featured a polypropylene separator, specifically Celgard 2400, to prevent direct contact between the anode and cathode while allowing for ion transport. Electrochemical impedance spectroscopy (EIS) analyses were conducted using an VMP-300 electrochemical workstation provided by Bio-Logic Co., Ltd. The EIS tests spanned a frequency range from 100 mHz to 100 kHz, applying a perturbation amplitude of 5 mV across the electrodes. The electrochemical performance evaluation was carried out using a NEWARE battery analyzer, a product of NEWARE Technology Ltd. based in Shenzhen, China. Cycling stability was assessed through stripping/plating experiments on symmetric cells. These cells were constructed with lithium foil and PFDTMS@Li electrodes, and tested at current densities of 0.5 mA cm^{-2} . Each cycle encompassed a specific capacity of 0.5 mAh cm^{-2} . The electrolyte utilized in these experiments comprised 1 M lithium hexafluorophosphate (LiPF_6) dissolved in a 3:7 (by volume) mixture of ethylene carbonate (EC) and ethyl methyl carbonate (EMC) augmented with 1 wt % lithium difluoro(oxalate)borate (LiDFOB) to improve electrolyte properties.

Materials Characterization. SEM Analysis: Sample morphology was assessed using a Hitachi S-4800 SEM at 3 kV. Samples, including PFDTMS@Li and Li foil electrodes, were transferred under inert conditions from a glovebox to the SEM chamber via a custom-built, airtight transfer device to prevent exposure to ambient air. XPS Analysis: X-ray Photoelectron Spectroscopy (XPS) spectra were acquired with a Thermo Scientific ESCALAB 250Xi instrument, employing monochromated Al K α radiation at 200 W. Samples were transferred in an argon atmosphere from the glovebox to the XPS measurement chamber through a custom-designed, gastight XPS transfer chamber.

3. Results and Discussion

Figure 1(a) presents a schematic representation outlining the fabrication process

of PFDTMS@Li, where 0.2 grams of PFDTMS is dissolved in a 10 milliliter solution of tetrahydrofuran (THF), subsequently immersing lithium foils within this mixture for a duration of 10 hours. This allows for the autonomous deposition of PFDTMS onto the lithium metal surface, with the underlying reaction mechanism detailed in Equation (1). A visual inspection of the altered lithium surface reveals a notably smoother texture on the PFDTMS-treated lithium sheets, evidencing the effective coupling and formation of a conformal coating layer by PFDTMS on the metal lithium substrate. In **Figure 1(b)**, the molecular architecture of PFDTMS is depicted, highlighting its rich content of C-F and Si-O bonds. These bonds facilitate the creation of a robust solid electrolyte interphase (SEI) on the lithium metal surface, replete with LiF and Si-O-containing compounds, which collectively contribute to a marked improvement in the electrochemical performance characteristics of lithium-metal-based batteries. Lastly, **Figure 1(c)** showcases the X-ray photoelectron spectroscopy (XPS) Si2p profile of PFDTMS@Li, unambiguously exhibiting the presence of prominent Si-O bonds [13]. This observation further consolidates the notion that PFDTMS has indeed been successfully attached to the surface of the metal lithium, reinforcing the strategic modification aimed at enhancing battery performance and stability.

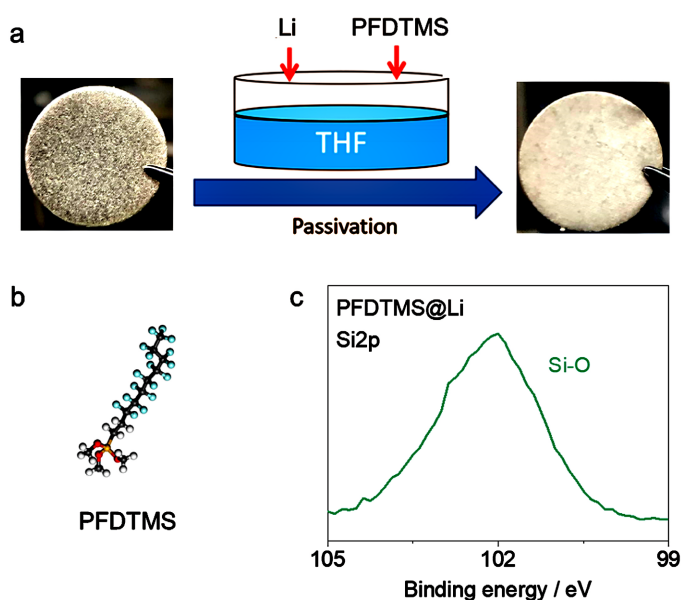


Figure 1. (a) Schematic illustration of the preparation of PFDTMS@Li, (b) Structural diagram of the PFDTMS molecule, (c) XPS Si2p spectrum of PFDTMS@Li.

The effect of the PFDTMS interfacial modification layer was evaluated using the cycling test of symmetric lithium cells. As shown in **Figure 2(a)**, when cycled at a current density and capacity density of 0.5 mA cm^{-2} and 0.5 mAh cm^{-2} respectively, bare Li experiences a rapid increase in polarization voltage after 300 hours, indicating polarization failure. Conversely, PFDTMS@Li only begins to show a gradual increase in polarization voltage after being cycled for 600 hours,

suggesting that the PFDTMS modification enhances the SEI on the lithium metal anode and suppresses side reactions at the interface. **Figures 2(b)-(c)** illustrate the electrochemical impedance of Bare Li and PFDTMS@Li before and after cycling, respectively. The initial impedance of the symmetric cell is higher for PFDTMS@Li compared to uncoated Li due to the thicker interphase formed after PFDTMS coating. Nevertheless, because of the high-performance interfacial layer, PFDTMS@Li exhibits significantly reduced impedance after cycling compared to bare Li. These results from the symmetric cell tests indicate that PFDTMS, when used as an interfacial modifier for metallic lithium, effectively inhibits side reactions between the lithium metal and the electrolyte, thereby enhancing the interfacial stability of the lithium metal anode.

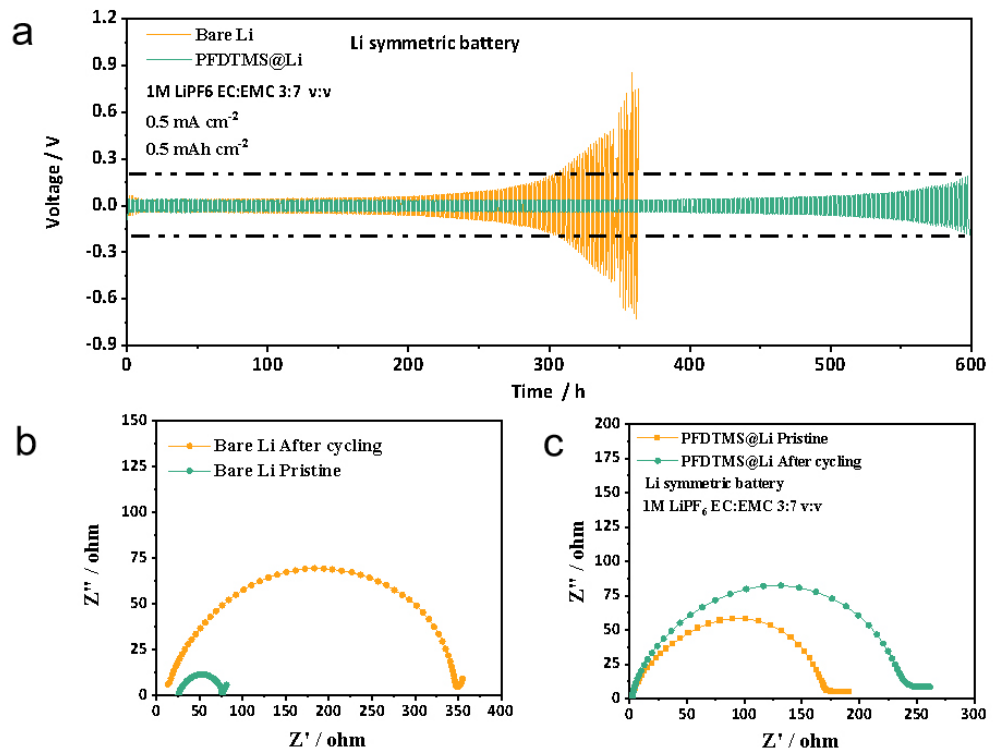


Figure 2. (a) Time-voltage profiles of Li||Li symmetric cells, (b) Electrochemical impedance before and after cycling of bare Li, (c) Electrochemical impedance before and after cycling of PFDTMS@Li.

In order to better evaluate the functionality of PFDTMS as an interfacial modifier, we observed the deposition morphology on the lithium metal surface via SEM to gauge the effectiveness of the interface modification. As depicted in **Figures 3(a)-(b)**, which show the initial deposition morphologies of Bare Li and PFDTMS@Li respectively, the surface of Bare Li exhibits numerous dendritic formations, whereas PFDTMS@Li displays predominantly block-like lithium deposits, indicating that the PFDTMS modification layer effectively suppresses dendrite formation. With the aim to improve the performance of lithium metal batteries, PFDTMS-modified lithium was utilized to assemble Li//NMC811 cells for cycling tests. **Figure 3(c)** presents the first charge-discharge curves of Li//NMC811

cells, revealing a higher coulombic efficiency for PFDTMS@Li compared to Bare Li. This suggests that PFDTMS, serving as an interfacial modifier, can inhibit side reactions between the electrolyte and the metal lithium, consistent with the outcomes observed in symmetric cell testing. **Figure 3(d)** illustrates the cycling performance of Li//NMC811 batteries, demonstrating improved performance by PFDTMS@Li due to the protection it affords to the metal lithium. Collectively, these results affirm that PFDTMS, when employed as an interfacial modifier layer, effectively protects the lithium metal anode and enhances the cycling performance of lithium metal batteries.

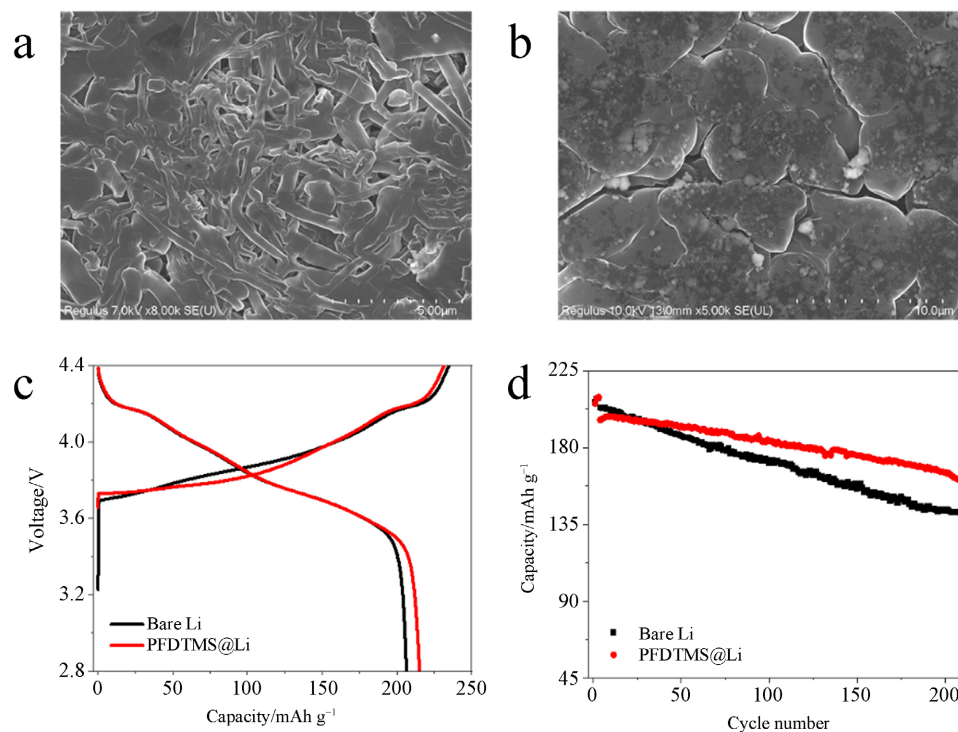


Figure 3. (a) SEM image of Bare Li, (b) SEM image of PFDTMS@Li, (c) Initial charge-discharge curves of Li||NMC811, (d) Cycling performance of Li||NMC811.

4. Conclusion

In this work, we employed molecular self-assembly techniques to introduce a PFDTMS modification layer on the surface of lithium metal anodes, effectively suppressing side reactions between the metal lithium and electrolyte, thereby significantly improving the cycling performance of lithium metal batteries. The modified lithium metal battery retains a capacity retention rate of 82% after 200 cycles, while the unmodified lithium metal battery only retains 69%. Our research offers the advantages of low cost and simplicity, presenting promising application prospects and providing valuable insights for interfacial protection strategies in other secondary battery systems. The high-energy-density batteries we have fabricated are capable of minimizing the quantity of raw materials needed for their production, which in turn leads to reduced manufacturing ex-

penses. Additionally, by decreasing the environmental impact associated with discarded batteries, these advancements promote a more sustainable approach to energy storage and usage. This not only benefits the economy by lowering costs but also addresses pressing environmental concerns related to waste management and resource depletion, aligning well with global sustainability goals.

Conflicts of Interest

The author declares no conflicts of interest regarding the publication of this paper.

References

- [1] Xu, W., Wang, J., Ding, F., Chen, X., Nasybulin, E., Zhang, Y., *et al.* (2014) Lithium Metal Anodes for Rechargeable Batteries. *Energy & Environmental Science*, **7**, 513-537. <https://doi.org/10.1039/c3ee40795k>
- [2] Cheng, Y., Ke, X., Chen, Y., Huang, X., Shi, Z. and Guo, Z. (2019) Lithiophobic-Lithiophilic Composite Architecture through Co-Deposition Technology toward High-Performance Lithium Metal Batteries. *Nano Energy*, **63**, Article 103854. <https://doi.org/10.1016/j.nanoen.2019.103854>
- [3] Lei, D., Shi, K., Ye, H., Wan, Z., Wang, Y., Shen, L., *et al.* (2018) Progress and Perspective of Solid-State Lithium-Sulfur Batteries. *Advanced Functional Materials*, **28**, Article 1707570. <https://doi.org/10.1002/adfm.201707570>
- [4] Wang, Y., Wang, Z., Lei, D., Lv, W., Zhao, Q., Ni, B., *et al.* (2018) Spherical Li Deposited inside 3D Cu Skeleton as Anode with Ultrastable Performance. *ACS Applied Materials & Interfaces*, **10**, 20244-20249. <https://doi.org/10.1021/acsami.8b04881>
- [5] Wang, Z., Wang, Y., Zhang, Z., Chen, X., Lie, W., He, Y., *et al.* (2020) Building Artificial Solid-Electrolyte Interphase with Uniform Intermolecular Ionic Bonds toward Dendrite-Free Lithium Metal Anodes. *Advanced Functional Materials*, **30**, Article 2002414. <https://doi.org/10.1002/adfm.202002414>
- [6] Hou, C., Han, J., Liu, P., Yang, C., Huang, G., Fujita, T., *et al.* (2019) Operando Observations of SEI Film Evolution by Mass-Sensitive Scanning Transmission Electron Microscopy. *Advanced Energy Materials*, **9**, Article 1902675. <https://doi.org/10.1002/aenm.201902675>
- [7] Zhang, H., Eshetu, G.G., Judez, X., Li, C., Rodriguez-Martínez, L.M. and Armand, M. (2018) Electrolyte Additives for Lithium Metal Anodes and Rechargeable Lithium Metal Batteries: Progress and Perspectives. *Angewandte Chemie International Edition*, **57**, 15002-15027. <https://doi.org/10.1002/anie.201712702>
- [8] Song, J., Lee, H., Choo, M., Park, J. and Kim, H. (2015) Ionomer-Liquid Electrolyte Hybrid Ionic Conductor for High Cycling Stability of Lithium Metal Electrodes. *Scientific Reports*, **5**, Article No. 14458. <https://doi.org/10.1038/srep14458>
- [9] Xie, J., Liao, L., Gong, Y., Li, Y., Shi, F., Pei, A., *et al.* (2017) Stitching h-BN by Atomic Layer Deposition of LiF as a Stable Interface for Lithium Metal Anode. *Science Advances*, **3**, eaao3170. <https://doi.org/10.1126/sciadv.aao3170>
- [10] Lin, D., Liu, Y., Chen, W., Zhou, G., Liu, K., Dunn, B., *et al.* (2017) Conformal Lithium Fluoride Protection Layer on Three-Dimensional Lithium by Nonhazardous Gaseous Reagent Freon. *Nano Letters*, **17**, 3731-3737. <https://doi.org/10.1021/acs.nanolett.7b01020>

-
- [11] Cheng, Q., Li, A., Li, N., Li, S., Zangiabadi, A., Li, T., *et al.* (2019) Stabilizing Solid Electrolyte-Anode Interface in Li-Metal Batteries by Boron Nitride-Based Nanocomposite Coating. *Joule*, **3**, 1510-1522. <https://doi.org/10.1016/j.joule.2019.03.022>
- [12] Li, N., Yin, Y., Yang, C. and Guo, Y. (2015) An Artificial Solid Electrolyte Interphase Layer for Stable Lithium Metal Anodes. *Advanced Materials*, **28**, 1853-1858. <https://doi.org/10.1002/adma.201504526>
- [13] Wang, Y., Wang, Z., Zhao, L., Fan, Q., Zeng, X., Liu, S., *et al.* (2021) Lithium Metal Electrode with Increased Air Stability and Robust Solid Electrolyte Interphase Realized by Silane Coupling Agent Modification. *Advanced Materials*, **33**, Article 2008133. <https://doi.org/10.1002/adma.202008133>